Title: Compensatory changes in GABAergic inhibition are differentially expressed in the respiratory network to promote function following hibernation

Authors: Sandy E Saunders[1] & Joseph M. Santin[1]

[1]University of Missouri-Columbia, Missouri, United States of America.

*Corresponding authors' email: Sesf8g@missouri.edu, santinj@missouri.edu

Key words: GABAergic inhibition, neuroplasticity, compensation, control of breathing

Abstract

The respiratory network must produce consistent output throughout an animal's life. Although respiratory motor plasticity is well appreciated, how plasticity mechanisms are organized to give rise to robustness following perturbations that disrupt breathing is less clear. During underwater hibernation, respiratory neurons of bullfrogs remain inactive for months, providing a large disturbance that must be overcome to restart breathing. As a result, motoneurons upregulate excitatory synapses to promote the drive to breathe. Reduced inhibition often occurs in parallel with increased excitation, yet the loss of inhibition can destabilize respiratory motor output. Thus, we hypothesized that GABAergic inhibition would decrease following hibernation, but this decrease would be expressed differentially throughout the network. We confirmed that respiratory frequency was under control of $GABA_AR$ signaling, but after hibernation, it became less reliant on inhibition. The loss of inhibition was confined to the respiratory rhythm-generating centers: non-respiratory motor activity and large seizure-like bursts were similarly triggered by $GABA_A$ receptor blockade in controls and hibernators. Supporting reduced presynaptic GABA release, firing rate of respiratory motoneurons was constrained by a phasic $GABA_AR$ tone, but after hibernation, this tone was decreased despite the same postsynaptic receptor strength as controls. Thus, selectively reducing inhibition in respiratory premotor networks promotes stability of breathing, while wholesale loss of $GABA_ARs$ causes non-specific hyperexcitability throughout the brainstem. These results suggest that different parts of the respiratory network select distinct strategies involving either excitation (motoneurons) or inhibition (rhythm generator) to minimize pathological network states when engaging plasticity that protects the drive to breathe.

Introduction

Neuroplasticity is critical in neural systems to ensure the maintenance of function in an ever-changing environment. The neural circuit that generates breathing is no exception, as it is highly plastic and must respond appropriately to the environment of the organism for survival. In the respiratory control system, plasticity can function through a variety of feedforward (Mitchell et al., 2001; Herman et al., 2004) and feedback mechanisms (Mahamed et al., 2011; Baertsch and Herman, 2013; Streeter and Baker-Herman, 2014). In the case of feedforward plasticity, such as long-term facilitation of motor output following intermittent hypoxia, these mechanisms can promote “learning” in respiratory network. On the other hand, feedback mechanisms appear to protect the drive to breath by stabilizing motor output in response to environmental perturbations. Along these lines, respiratory motor inactivity in different vertebrate species triggers plasticity that can compensate for this disturbance to restore respiratory activity (Streeter and Baker-Herman, 2014; Brown et al., 2016; Santin, 2019). To date, most mechanistic work has focused on excitatory synapses of motoneurons as targets of such plasticity; however, alterations in fast synaptic inhibition are often triggered by changes in neuronal activity in a variety of different neural systems (Benevento et al., 1995; Hendry et al., 1994; Hendry & Jones, 1986, 1988; Rutherford et al., 1997; Hartman et al., 2006; Kilman et al., 2002). In the breathing network, GABAergic inhibitory plasticity has been shown to compensate in part for exposure to teratogens like nicotine during development (Pilarski and Fregosi, 2009; Wollman et al., 2022; Delhaes et al., 2014) but how inhibitory neuroplasticity functions to maintain respiratory activity in adults is poorly understood (Braegelmann et al., 2017).

Although alterations in synaptic inhibition co-occur with changes in excitation during activity disturbances, compensatory changes in inhibition have the potential to cause maladaptive outcomes for network performance. On the one hand, reducing inhibition could serve to boost respiratory motor output because decreases in inhibition can increase motor amplitude (Baertsch et al., 2018; Janczewski et al., 2013; Saunders and Santin, 2023). On the other hand, altering the normal inhibitory tone could be detrimental for breathing. Indeed, inhibition plays a variety of roles in respiratory pattern formation, including maintaining proper timing and coordination of respiratory motor

pools (Barnett et al., 2018), with loss of inhibition often presenting as loss of sequential patterning with increased motor synchrony (Kimura et al., 1997; Anderson et al., 2016; Büsselberg et al.,2001). In addition, inhibition contributes to normal respiratory motor burst shape, amplitude, and frequency, functioning in part to promote a large scope for increases in motor output in response to various stimuli, such as hypercapnia (Baertsch et al., 2018, Cregg at al., 2017; Zuperku and McCrimmon, 2002). Given the diverse roles of inhibition in the respiratory network, how plasticity acts through inhibition to ensure breathing remains stable in response to perturbation is unclear.

To investigate plasticity of the GABA system in the adult respiratory network, we took advantage of an extreme model of respiratory neuroplasticity—hibernation in the American bullfrog. These animals use lungs for gas exchange and contain all salient components of the respiratory network, including a respiratory rhythm generator (Wilson et al., 2002; Baghdadwala et al., 2015; Baghdadwala et al., 2016), central chemoreceptors (Amaral-Silva and Santin, 2023b; Burton and Santin 2020; Santin and Hartzler, 2013), and conserved nuclei for sensory integration (Hanamori et al., 1987; Wang et al., 1999). However, during hibernation they may spend up to several months under water without access to air using only skin to breathe. As a result, respiratory motor neurons, and potentially the rest of the network, remain inactive (Santin & Hartzler, 2017). Instead of atrophying like other muscles and motoneurons during periods of inactivity (Banzrai et al., 2016; Cormery et al., 2006; Langlet et al., 2012; Fahim, 1989), including mammals on mechanical ventilation (Smuder et al., 2023), a suite of compensatory mechanisms ensures functional breathing after hibernation in the spring (Santin & Hartzler, 2016, Santin, 2019). Specifically, motoneurons increase the strength of AMPA-glutamate receptor currents and maintain the capacity for high frequency firing to promote respiratory motor outflow (Santin et al., 2017, Zubov et al., 2022). Given the complex role that inhibition plays within the respiratory network, and the typical trend toward reduced inhibition with inactivity, we hypothesized that compensatory decreases in inhibition would occur where the loss of inhibition is tolerated functionally. We tested this hypothesis at different levels of organization to provide insights into where inhibitory compensation occurs in the respiratory network. To determine compensatory changes to network level GABAergic neurotransmission, we

tested the sensitivity of rhythmic brainstem-spinal cord preparations to muscimol and bicuculline, $GABA_A$ receptor agonists and antagonists, respectively. We next used a novel semi-intact preparation to record respiratory motor neurons receiving respiratory input from the rhythm-generating circuit, isolating the GABAergic tone of individual motoneurons bursting in phase with the respiratory motor output. Finally, we recorded identified motoneurons in isolated brain slices to determine compensatory changes in post-synaptic inhibitory neurotransmission.

Materials and Methods

Animals

All experiments performed were approved by the Institutional Animal Care and Use Committee (IACUC) at the University of Missouri (protocol #39264). Adult Female American Bullfrogs (~100 g weight, n= 46), *Lithobates catesbeianus*, were purchased from Rana Ranch (Twin Falls, Idaho) and were housed in 20-gallon plastic tanks containing dechlorinated water at room temperature bubbled with room air. Control frogs were acclimated for 1 week following arrival before experiments. Frogs had access to wet and dry areas. Frogs were maintained on a 12-hour light/dark cycle and fed once per week. Water was cleaned daily and changed weekly. Hibernated frogs were kept in plastic tanks under the same conditions (exception of food being withheld) as control frogs for > 1 week before temperature was gradually lowered to 4°C over 10 days in a walk-in temperature-controlled environmental chamber. Once water temperature reached 4°C, air access was blocked using a plastic screen placed in the tank. After 4 weeks of submergence, experiments commenced.

Drugs

Strychnine hydrochloride was from Sigma-Aldrich (St Louis, MO, USA). (-)-Bicuculline methiodide, Tetrodotoxin citrate, DNQX disodium salt, and Muscimol were from Hello Bio (Princeton, NJ, USA).

Brainstem-spinal cord preparation

Brainstem-spinal cord preparations were generated as previously described (Burton and Santin, 2020). Briefly, frogs were deeply anesthetized with isoflurane until visible respirations had ceased and response to foot pinch was absent. Frogs were then decapitated with a guillotine. The head was submerged in ice-cold bullfrog artificial cerebrospinal fluid (aCSF; concentrations in [mM]: 104 NaCl, 4 KCl, 1.4 $MgCl_2$, 7.5 glucose, 40 $NaHCO_3$, 2.5 $CaCl_2$ and 1 NaH_2PO_4, and gased with 98.5% O_2, 1.5% CO_2; pH = 7.85) and the forebrain was pithed. The brainstem-spinal cord was then carefully removed, keeping nerve roots intact. Following the dissection, the brainstem was transferred to a chamber superfused with oxygenated aCSF. In a subset of experiments

where bicuculline was bath applied to the in vitro preparation (described below), brainstems were transected at the spinomedullary junction before recording. Cranial nerve X (vagus) activity was recorded using glass suction electrodes immediately following dissection. Recordings were AC amplified (1000x, A–M Systems Model 1700, A–M Systems, Carlsborg, WA, USA), filtered (10 Hz – 5 kHz), and digitized (Powerlab 8/35 ADInstruments, Colorado Springs, CO, USA). Nerve activity was rectified and integrated (time constant =100 ms) online to allow for visualization of nerve output pattern.

Vagus nerve output was then allowed to stabilize for ≥ 1 hour before drug application. In a subset of experiments (n=10 bullfrogs), various does of bicuculline (500 nM, 1 μM, 5 μM, 10 μM), a $GABA_A$ receptor antagonist, were superperfused for 10 minutes in order of increasing concentration and then washed out. In a different subset of experiments (n=10 bullfrogs), various doses (500 nM, 1 μM, 3 μM) of muscimol, a $GABA_A$ receptor agonist, were added to the perfusate. Each dose was superperfused for 10 minutes in order of increasing concentration. Bicuculline (10 μM) was added to the perfusate following muscimol to reverse muscimol's effects serving as a control that output depression was not due to preparation drift but rather activation of $GABA_A$ receptors.

Dye labeling of vagal motor neurons

Brainstems were isolated as described above. In a different group of experiments, following isolation, brainstems were transferred to a chamber superfused with oxygenated aCSF. The 4th branch of the vagal nerve root, which largely innervates the glottal dilator (Kogo and Remmers, 1994; Kogo et al., 1994; Sakakibara, 1984), was then isolated and suctioned into a glass pipette (bilaterally). Fluorescent dextran dye dissolved in PBS (tetramethylrhodamine 3000 MW lysine fixable dye; Invitrogen – Thermo Fisher, Waltham, MA, USA) was then backfilled into both pipettes and left to diffuse into the nerve root for 2 hours. This generated robust labeling of vagal motor neurons as previously described (Santin et al., 2017).

Semi intact Brainstem-spinal cord preparation

Following dye labelling, in a subset of experiments (n=15 bullfrogs) the brainstem was embedded into agarose and sliced, similar to previously described (Amaral-Silva and Santin, 2022) with some modifications. Briefly, partially cooled, but not solidified, agarose was pipetted into a thin layer onto a scored (with fine forceps) agar block. The brainstem was then dragged onto the agarose-covered agar block, laying horizontally dorsal side up. Agarose (~57˚ C) was the pipetted onto the top of the brainstem caudal to obex. The agar block was then mounted on a vibrating microtome plate (Campden Vibrating Microtome 7000smz, Campden Instruments; Lafayette, IN, USA) and covered in ice-cold bubbled aCSF. The blade was zeroed at the top of the brainstem, then slices were taken caudal to rostral, stopping shortly rostral to obex which was approximately 1/3 of the distance from the hypoglossal root to the vagal root. The blade was removed after each slice and the resulting attached slice was trimmed off the brainstem with fine spring scissors. Approximately 650 microns were removed from the dorsal surface in total, providing access to labelled motor neurons for recording. The brainstem was removed from the remaining agar and transferred to a 35mm glass bottom sylgard-coated dish with a stainless-steel mesh insert. The brainstem was then pinned dorsal side up. The dish was placed in a QE-1 platform (Warner Instruments, Holliston, MA, USA) that mounted on a fixed stage microscope (FN1, Nikon Instruments Inc., Melville, NY, USA). Once on the rig, the preparation was superperfused with bubbled aCSF either using gravity or with a peristaltic pump (Rainin Rabbit). The trigeminal nerve (CN V) was recorded using a glass suction electrode to monitor preparation output over time. Nerve recordings were AC amplified (1000x, A–M Systems Model 1700, A–M Systems, Carlsborg, WA, USA), filtered (10 Hz – 5 kHz), and digitized (Powerlab 8/35 ADInstruments, Colorado Springs, CO, USA). The trigeminal nerve was recorded instead of the vagal nerve root because of physical constraints in the bath with the patch pipette and picrospritzer pipette used in experiments described below. Labelled motor neurons were then located and visualized using an imaging camera (Hamamatsu ORCA Flash 4.0LT sCMOS, Hamamatsu Photonics, Hamamatsu City, Japan) coupled to Nikon imaging software (NIS elements).

Whole-cell recordings were made from labelled motor neurons with an Axopatch 200B amplifier (Molecular Devices) in current-clamp mode (I=0). Cells were selected based on firing pattern, that is only cells with bursting or an increase in spontaneous activity during respiratory bursts were sampled, as these neurons likely innervate the glottal dilator of bullfrogs, which is critical to permit airflow into the lungs of bullfrogs during ventilation and as such remains inactive during hibernation. Accordingly, neurons with subthreshold respiratory input or neurons that were active only during the interburst interval were excluded from testing. Glass pipettes (~4-7 MΩ) were filled with a solution containing (in mmol): 110 potassium gluconate, 2 $MgCl_2$, 10 Hepes, 1 Na_2-ATP, 0.1 Na_2-GTP and 2.5 EGTA, pH ~ 7.2 with KOH. Data were acquired in pClamp 11 software using an Axopatch 200B amplifier and Axon Digidata 1550B digitizer (Molecular Devices, San Jose, CA, USA). To determine inhibitory tone onto respiratory motor neurons, bicuculline (50 μM) was focally applied using a Picospritzer II (General Valve Corporation, Fairfield, NJ, USA) to the recorded cell following a baseline period (≥10 respiratory bursts). Bicuculline was applied using a 5 sec pulse, every 10 secs for 5-10 minutes. A washout period was used to verify changes in cell firing frequency were due to drug application and not cell drift. Changes in firing frequency during bicuculline application and wash were rapid, suggesting the area was saturated with drug upon administration and then quickly washed. In a subset of cells where a gigaohm seal was not formed, recordings of neuronal firing rate were performed in the loose-patch configuration (V_{hold}=0 mV; n=2 in control, and n=2 in hibernation). All voltages from current-clamp experiments were corrected for a liquid junction potential of 12 mV.

Brain Slice electrophysiology

Following dye labelling, in a subset of experiments brainstem slices (300 μm) containing labeled motor neurons were obtained (n=11 bullfrogs). Whole-cell recordings were made from labelled motor neurons with an Axopatch 200B amplifier (Molecular Devices) in voltage clamp (V_{hold}=-60 mV) mode. Glass pipettes (2.6-4 MΩ) were filled with a solution containing (in mmol): 95 CsCl, 2 $MgCl_2$, 10 Hepes, 1 Na_2-ATP, 0.1 Na_2-GTP, 10 EGTA, 1 $CaCl_2$ and 10 tetraethylammonium-Cl (TEA), pH ~ 7.2 using CsOH. Data were acquired in pClamp 11 software using an Axopatch 200B amplifier and Axon Digidata

1550B digitizer (Molecular Devices, San Jose, CA, USA). To examine miniature inhibitory postsynaptic currents (mIPSCs), tetrodotoxin (TTX; 250 nM) and DNQX (10 μM) were bath applied for 3 min to block voltage-gated Na^+ channels and AMPA receptors. Strychnine (5 μM) was then bath applied in combination with TTX and DNQX for 2 min to block glycingeric mIPSCs and isolate GABAergic mIPSCs which were recorded for 1 min. All GABAergic mIPSCs were blocked following perfusion of bicuculline (50 μM) confirming their isolation. A voltage step was performed at the beginning of each recording and before each solution change to monitor series resistance (R_s; estimated from the transient) and input resistance (R_{IN}; estimated from the steady state). R_s was not compensated but remained <25 MΩ for inclusion.

Data Analysis

For experiments using the intact brainstem preparation, burst frequency was determined from integrated vagus nerve signals using the peak analysis function in LabChart 8 (ADInstruments Inc., Colorado Springs, CO, USA). Burst start and stop timepoints were defined as 5% of the height from baseline. In experiments where muscimol was systemically applied, data were sampled from the last 3 minutes of each condition (baseline, 500 nM, 1 μM, and 3 μM). In experiments where bicuculline was systemically applied, data were sampled for 10 minutes during each condition (baseline, 500 nM, 1 μM, 5 μM, 10 μM). In experiments where non-respiratory bursting was quantified, non-respiratory bursts were counted manually.

For experiments using the semi-intact preparation, action potentials were detected with the peak analysis function in LabChart 8 (ADInstruments Inc., Colorado Springs, CO, USA). Following detection of action potentials, a channel was created that plotted firing frequency over time. Average firing frequency per respiratory burst was determined via the mean firing frequency from neuronal burst start to stop. Average firing frequency was sampled and averaged from 10 respiratory bursts in each condition (baseline, bicuculline, and wash).

For voltage-clamp experiments in brainstem slices, average amplitude (current measurement from baseline to peak), charge transfer (integral of the mIPSC), rise time

(time from baseline to peak), and frequency of GABAergic mIPSCs (mIPSC/sec) were analyzed from one minute of gap free recording following two minutes of exposure to TTX/DNQX/Strychnine (as described above) using the peak analysis function in LabChart 8 (ADInstruments Inc., Colorado Springs, CO, USA). Events below 7.5 pA were excluded. Events were inspected manually to ensure the accurate detection of mIPSCs. For construction of the cumulative probability histogram, the first 50 mIPSCs from the minute of data obtained from each neuron were sampled.

Statistics

Data are presented as mean ± s.d. unless otherwise stated. When two groups of dependent samples were compared ("before-after" experiments), a two-tailed paired t-test was used. When two groups of independent samples were compared, a two-tailed unpaired t-test was used. In experiments with two main effects, a two-way ANOVA was used. Two-way ANOVA were followed up with Holm-Šidák multiple comparisons test, unless otherwise specified. Cumulative distributions were compared with the Kolmogorov-Smirnov test. Significance was accepted when $P < 0.05$. All analyses were performed using GraphPad Prism (v9.4.1, San Diego, CA, USA).

Results

To investigate inhibitory tone at the network level, bicuculline, a $GABA_A$ receptor antagonist, was bath-applied to intact brainstem preparations from control and hibernated bullfrogs (Figure 1). Similar to brainstem preparations from adult bullfrogs shown in Broch et al., 2002, bicuculline caused a dose-dependent decrease in respiratory burst frequency (Figure 1A), with most control preparations having little or no respiratory bursting at the highest dose of bicuculline (Baseline Frequency: 42.6 ± 16.3 bursts/min; Frequency at 10 μM: 1.7 ± 1.1 bursts/min; n=5; Figure 1C). Motor output from hibernators was much more resistant to bath application of bicuculline (Figure 1B). Accordingly, respiratory bursting persisted even at the highest doses in preparations from hibernated animals (Frequency at 10 μM: 13.5 ± 4.1 bursts/min; n=5; Figure 1C), unlike respiratory bursting from control preparations. Interestingly, the frequency of non-respiratory bursting dose-dependently increased following bicuculline administration in preparations from both hibernated and control animals (Figure 1D). Furthermore, higher doses of bicuculline often led to large motor bursts (> 30 sec duration; “seizure-like”) characterized by increases in tonic background nerve activity with 5 μM bicuculline promoting these bursts in the majority of preparations from both groups (4 out of 5 controls; 3 out of 5 hibernated). Taken together, the respiratory network after hibernation has a lower reliance on $GABA_AR$ signaling to control network frequency, while the ability for reduced inhibition to induce non-respiratory bursting and seizure-like activity was similar across groups.

We then performed experiments to determine if respiratory motor output would be more resistant to depression induced by $GABA_AR$ agonists following hibernation. To test this, muscimol, a $GABA_AR$ agonist, was bath-applied to intact brainstem preparations from controls and hibernators (Figure 2A). Respiratory burst frequency was unchanged by 500 nM muscimol (Baseline, 8.27 ± 3.7 bursts/min vs 500 nM muscimol, 7.20 ± 4.0 bursts/min; n=5) but was significantly reduced following bath application of 1 μM muscimol (1 μM muscimol, 3.47 ± 1.9 bursts/min; p= 0.0282; n=5; Figure 2C). Increasing the dose of muscimol to 3 μM silenced output from all control preparations (5 out of 5). In contrast, in preparations from hibernators (Figure 2B), there was no significant difference in respiratory burst frequency between baseline and any

dose of muscimol (Baseline, 11.00 ± 2.1 bursts/min; 500 nM muscimol, 11.93 ± 1.8 bursts/min; 1 μM muscimol, 14.47 ± 2.8 bursts/min; 3 μM muscimol, 6.47 ± 7.3 bursts/min; n=5; Figure 2C). This effect was similarly observed when normalizing burst frequency to baseline (Figure 2D). Thus, brainstem respiratory output from hibernators was remarkably insensitive to muscimol-mediated suppression of burst frequency.

The changes we observed in sensitivity of respiratory frequency to depression suggest that hibernation reduces GABA signaling within the rhythm-generating network. However, given that we previously showed compensation through excitatory synapses occurs at the motoneuron, we next sought to determine if changes in inhibitory tone happened in the premotor circuit or motoneurons themselves. To test this, vagal respiratory motor neurons were recorded in a semi-intact preparation that maintains rhythmic motor output that is similar to output observed in the intact brainstem preparation and *in vivo* (Figure 3A). This activity reflects motoneurons firing in response to respiratory-related excitation from presynaptic circuits, as well as inhibition that shapes the respiratory motor burst. At baseline, dye-labeled vagal motor neurons fired spontaneous bursts of action potentials during the respiratory motor burst as well during occasional non-respiratory bursts (Figure 3A, 3B).

To determine the GABAergic inhibitory tone on these neurons, action potentials during respiratory-related bursts in current-clamp (I=0) or sometimes in loose patch configuration (V_{hold}=0 mV) were recorded before during and after focal application of bicuculline, a $GABA_AR$ antagonist. At baseline, motor neurons from both groups had similar average burst firing rates and resting membrane potential (Figure 3C). Local application of bicuculline led to a significant increase in average burst firing frequency of motor neurons from the control group (Baseline, 45.26 ± 34.8 Hz; Bicuculline, 89.36 ± 61.4 Hz; $p<0.0001$; n=12; Figure 4A, 4C) but not the hibernated group (Baseline, 24.19 ± 23.0 Hz; Bicuculline, 38.75 ± 44.9 Hz; $p=0.2629$; n=9; Figure 4B, 4C). Accordingly, the bicuculline-mediated change in firing frequency was significantly greater in the hibernated group than the control (Figure 4D). The bicuculline-mediated increase in firing frequency was readily reversed following wash out in both groups (Figure 4C). Additionally, there was no change in resting membrane potential during focal application of bicuculline in either control (Baseline: -61.52 ± 4.6 mV; Bicuculline: -60.92 ± 4.9 mV;

n=10) or hibernated groups (Baseline: -59.24 ± 6.5 mV; Bicuculline: -59.53 ± 6.5 mV; n=7) suggesting a lack of $GABA_AR$-mediated tonic current. Taken together, motor neurons from control animals had larger bicuculline-mediated increases in burst firing frequency than motor neurons from hibernated animals. This suggests phasic inhibition is reduced at the level of the motor neuron following hibernation to compensate for inactivity and preserve motoneuron firing rates.

To determine if the hibernation-mediated change in inhibitory tone of respiratory motor neurons in the semi-intact preparation was mediated in part by changes in post-synaptic inhibitory strength or presynaptic GABA release, we recorded miniature inhibitory post synaptic currents (mIPSCs) in brainstem slices (Figure 5). Our expectation was that if the GABA tone was decreased at the motoneuron, we would observe decreases in mIPSCs, while if plasticity occurred presynaptically, mIPSCs would remain unchanged. Whole-cell voltage clamp recordings of vagal motor neurons revealed that GABAergic mIPSCs were nearly indistinguishable from control and hibernated animals (Figure 5A). As such, we did not observe changes in mIPSC frequency, average amplitude, charge transfer, and rise time (Figure 5C). Neuronal input resistance was also unchanged (Figure 5C). To determine if there were any shifts in the distribution of mIPSCs that were not captured in the average amplitude, cumulative probability distributions from control and hibernation groups were plotted. Indeed, we did not observe any shifts throughout the distribution (Figure 5B). Furthermore, we did not observe any outward currents upon addition of bicuculline to the bath, further supporting the lack of $GABA_AR$-mediated tonic current in these neurons. Taken together, our data suggest that post-synaptic inhibitory strength was unchanged following hibernation. Thus, the change in inhibitory tone we detected at the level of the motor neuron likely occurs within the rhythmic premotor circuits in a way that can alter phasic GABA release during respiratory-related input.

Discussion

Here we tested the hypothesis that GABAergic inhibitory neurotransmission would decrease in the respiratory network to compensate for inactivity during hibernation, much like we observed for excitatory synapses within motoneurons (Santin et al., 2017, Zubov et al., 2022). Indeed, we found that GABAergic inhibitory tone was decreased in the respiratory network, but this decrease occurred through presynaptic, and not postsynaptic mechanisms. Below we describe how organizing multiple compensatory plasticity mechanisms in this way promotes motor performance, and thus, reduces the possibility of pathological network states during activity challenges.

Synaptic compensation for inactivity

Neural systems use homeostatic forms of plasticity to maintain function in a changing environment. Prior studies have demonstrated that excitatory synapses are up-scaled following hibernation (Zubov et al., 2022; Santin et al., 2017) aligning with classic mechanisms of inactivity-induced homeostatic plasticity (Fong et al., 2015; Lambo and Turrigiano, 2013; Turrigiano et al., 1998). Although there is an abundance of research on excitatory mechanisms of homeostatic plasticity, much less is known about the role of inhibitory neurotransmission. Of the studies examining plasticity of synaptic inhibition, many have shown that neurons change mIPSC amplitude (Hartman et al., 2006; Kilman et al., 2002, Peng et al., 2010; Swanwick et al., 2006) to compensate for changes in activity. In contrast to these studies, we have found that although respiratory motor neurons have compensated for chronic inactivity by reducing the inhibitory tone of motoneurons, they have done so without decreases in mIPSC amplitude. Assuming that post-synaptic receptors are saturated by single vesicles during spontaneous release (Barberis et al., 2004), the lack of change in GABAergic mIPSC amplitude suggests that there were no obvious changes in post-synaptic $GABA_AR$ density following hibernation and the changes we observed occur via reductions in presynaptic GABA release.

In the experiments where bicuculine was focally applied to rhythmic motoneurons, the bicuculline-mediated increase in burst firing frequency was attenuated in brainstems from hibernated animals, implying inhibitory synaptic strength was decreased following hibernation. The lack of changes we observed in mIPSCs from

hibernated motoneurons suggest that these decreases in synaptic inhibition that modulate firing rate occur through presynaptic mechanisms, likely through decreases in GABA release. Although our results strongly suggest GABA release from presynaptic neurons has been reduced, it is difficult at present to parse out the variables that account for this outcome (e.g., altered quantal content during evoked stimulation, probability of release, reduced excitability of GABAergic neurons, etc.) because the location of the respiratory synapses that drive respiratory motor neuron bursting remains unknown and the specific populations of GABAergic neurons that regulate motoneuron firing in the frog brain are not yet characterized. Nonetheless, our data are consistent with a response that is mediated in a large part through pre-synaptic mechanisms. As detailed in the following section, decreased sensitivity to bicuculline and muscimol-mediated frequency decline in the intact circuit further supports that inhibition in premotor circuits decreases following hibernation.

Hibernation-induced changes in respiratory motor sensitivity to $GABA_AR$ agonists and antagonists

Breathing is generated by a network of neurons in the brainstem. Rhythm-generating populations produce the rhythm that is transmitted to premotor and/or motor neurons facilitating their rhythmic activity. As such, respiratory-associated vagal motor neurons require presynaptic input to burst (Amaral-Silva and Santin, 2023a), functioning as one of the final motor outputs of the respiratory circuit. In preparations from hibernators, frequency of rhythmic respiratory motor output was largely insensitive to depression by muscimol and, albeit counterintuitively, depression by bicuculline. In the breathing circuit, frequency of motor output is thought to be controlled by modulation of the respiratory rhythm generator (Baker-Herman and Mitchell, 2008; Blitz and Ramirez, 2002). Therefore, insensitivity of preparations in the hibernated group to muscimol-mediated and bicuculline-mediated respiratory frequency decline suggests that compensation that decreases inhibitory neurotransmission occurs presynaptic to the motoneuron at the level of the respiratory rhythm generator and/or populations that modulate the respiratory CPG. Interestingly, bicuculline-mediated decreases in respiratory burst frequency have been previously shown to occur in brainstem

preparations from adult bullfrogs but not tadpoles (Broch et al., 2002), suggesting GABAergic inhibitory tone contributes to baseline respiratory frequency in a stage-dependent manner. Previous work suggests that certain features of the respiratory network, such as CO_2 and O_2 sensitivity, can return to a juvenile-like state following hibernation (Santin and Hartzler, 2016), consistent with the concept that certain developmental traits are plastic rather than fixed (Burggren, 2020). Thus, our experiments further support the idea that hibernation-induced plasticity can manifest as a more juvenile-like respiratory network phenotype, with a respiratory CPG that is less dependent on inhibitory neurotransmission to maintain normal respiratory frequency. Perhaps one consequence of a compensatory decrease in inhibitory tone is that while it locks in a set respiratory frequency, it also makes the network overall less flexible and dynamic during respiratory stimuli (Cui et al., 2016).

Vertebrate motor neurons are often multifunctional, whereby a motor neuron participates in more than one behavior (Briggman and Kristan, 2008; Figure 3B). These behaviors are mediated by different inputs from premotor neurons. In the mammalian brainstem preparation, systemic disinhibition via bicuculline administration promotes non-respiratory bursting in cervical nerves (Brockhaus and Ballanyi; 2000). This non-respiratory bursting is thought to originate from some combination of hyperexcitability in motor pools and in non-respiratory premotor networks including spinal networks. However, it does not reflect hyperexcitable activity from the respiratory CPG (Brockhaus and Ballanyi; 2000; Panaitescu et al., 2013). To eliminate spinal input during bicuculline administration, we transected all brainstems exposed to bicuculline at the spinomedullary junction. Although we found a large difference in the sensitivity to respiratory bursting to bicuculline, we found no difference in frequency of non-respiratory bursting facilitated by bath application of bicuculline in preparations from control and hibernated bullfrogs. Therefore, compensation for motor neuron inactivity involved decreases in inhibition that were specific to respiratory premotor circuits and not other premotor networks in the brainstem. This differential compensation further supports the idea that homeostatic adaptations resulting from inactivity are synapse-specific and ultimately aimed to promote functional output from the network (Kim and Tsien; 2008).

Organizing multiple forms of compensation within the respiratory network

In the vertebrate respiratory network, inhibitory neurotransmission contributes to many aspects of breathing. Evidence suggests that synaptic inhibition is not required to generate the vertebrate respiratory rhythm but does play a key role in respiratory pattern formation (Johnson et al., 2002; Janczewski et al., 2013; Bongianni et al., 2006, 2016; Saunders and Santin, 2023). Synaptic inhibition also works to maintain antagonistic relationships of neuronal populations (Kimura et al., 1997; Sun et al., 2008; Anderson et al., 2016;) that participate in behaviors where sequential patterning is necessary for function. Our results suggest that phasic GABAergic inhibition during the respiratory burst contributes to maintenance of normal firing rates of respiratory motor neurons under normal circumstances (Fig 4), which could promote a dynamic range of firing frequency through adjustments in the degree of inhibition (Cui et al., 2016). With this diversity of functional roles in mind, one could postulate that inhibition is more necessary in some parts of the network for function (maintaining proper relationships with other motor pools) and more dispensable in other parts (rhythmogenesis), seeing as respiratory rhythmogenesis proceeds with little $GABA_AR$ tone after hibernation (Fig 1-2). Along these lines, many studies have suggested that changing the level of $GABA_ARs$ on the motor neuron is maladaptive and promotes dysfunctional motor output (Jaiswal et al., 2015; Wollman et al., 2018; Khristy et al., 2009; Paulose et al., 2009). Therefore, the lack of changes in $GABA_AR$ on the motoneuron as we observed may relate to the necessity of a “normal” postsynaptic $GABA_AR$ level or “set point” for motor neuron function. Supporting this assertion, when a large fraction of $GABA_ARs$ were blocked, seizure-like activity that disrupted the normal respiratory output occurred in controls and hibernators. On the other hand, the decrease in presynaptic inhibition we observed via altered sensitivity of the motor neuron firing in our experiments (Figure 4) may arise from decreases in inhibitory input from the respiratory rhythm generator where inhibition is, in part, dispensable for function. Perhaps, this decrease in inhibition at the level of the respiratory CPG works to increase resilience of respiratory output to ensure that breathing restarts following prolonged inactivity. Our previous work suggests that AMPA receptor-mediated excitatory neurotransmission increases at the level of the motor neuron but not the respiratory CPG (Santin et al., 2017), presumably due to the

necessity of “correct” AMPA-receptor mediated activity for respiratory rhythmogenesis (Pace and Del Negro; 2008). Taken together, compensatory plasticity in the respiratory system can be adaptive or maladaptive depending on the context (Dempsey and Morgan, 2015), and our experiments suggest that for compensation to be adaptive, the network must consider what is absolutely required and what is dispensable, ultimately employing plasticity where it is tolerated functionally.

Conclusions

In sum, we found that inhibitory neurotransmission was decreased in the respiratory network following hibernation, which causes an extreme degree of respiratory motor inactivity. This decrease was differentially expressed throughout the network, with the respiratory CPG losing reliance on $GABA_AR$ signaling for maintaining respiratory frequency following hibernation. In contrast, post-synaptic $GABA_AR$ activity of vagal motor neurons was unchanged following hibernation. Furthermore, we observed no change in bicuculline-mediated non-respiratory motor activity, suggesting compensatory changes in inhibition were specific to the respiratory network. We suggest this differential inhibitory compensation is due to the relative dispensability of inhibition for certain functions. Importantly, the decrease in inhibition in the respiratory CPG likely comes at a cost, potentially including reduced dynamic range of network outputs. We propose compensatory mechanisms that preserve function could follow some hierarchical rule, whereby certain plasticity mechanisms are used only at specific network locations to promote healthy network performance.

Competing Interests: No competing interests declared.

Funding: This work was supported by the National Institutes of (R01NS114514 to JS) and laboratory start-up funds from The University of Missouri (to JS).

Figure 1

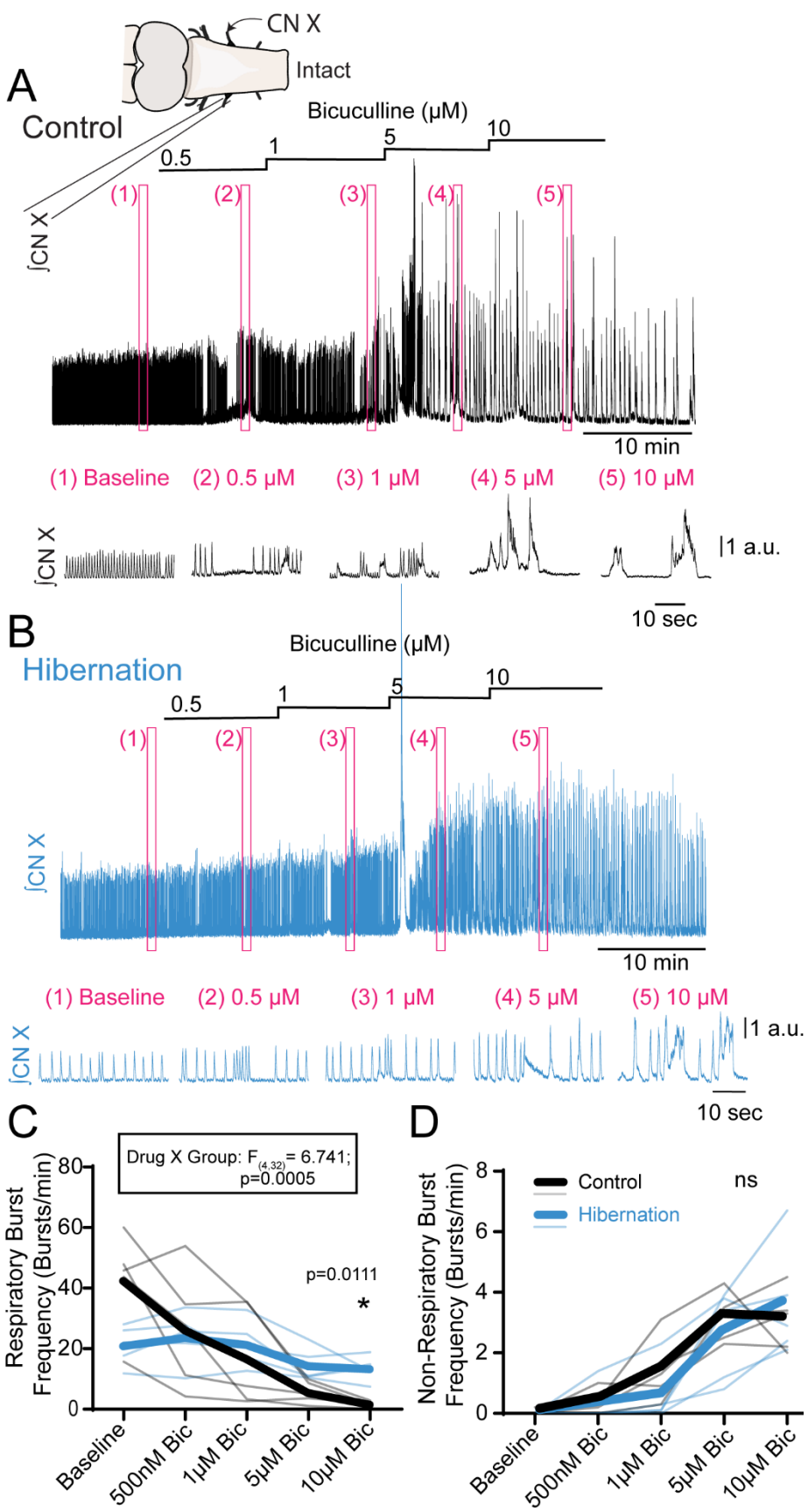
A
Control
CN X
Intact
Bicuculline (μM)
0.5
1
5
10
(1)
(2)
(3)
(4)
(5)
∫CN X
10 min
(1) Baseline
(2) 0.5 μM
(3) 1 μM
(4) 5 μM
(5) 10 μM
1 a.u.
10 sec
B
Hibernation
Bicuculline (μM)
0.5
1
5
10
(1)
(2)
(3)
(4)
(5)
∫CN X
10 min
(1) Baseline
(2) 0.5 μM
(3) 1 μM
(4) 5 μM
(5) 10 μM
1 a.u.
10 sec
C
Drug X Group: F(4,32) = 6.741; p=0.0005
p=0.0111
*
Respiratory Burst Frequency (Bursts/min)
0
20
40
60
80
Baseline
500nM Bic
1μM Bic
5μM Bic
10μM Bic
D
Control
Hibernation
ns
Non-Respiratory Burst Frequency (Bursts/min)
0
2
4
6
8
Baseline
500nM Bic
1μM Bic
5μM Bic
10μM Bic

Figure 1

GABAergic tone that controls normal respiratory burst frequency is decreased following hibernation. Integrated vagus nerve activity (CN X) was rhythmic in brainstem preparations from control and hibernated animals. A) Top, continuous recording of CNX during perfusion of increasing doses of bicuculline in a control preparation (black). Bottom, zoomed in view of epochs (pink boxes) indicated in continuous trace directly above. In control preparations, bath application of bicuculline led to a dose dependent decrease in respiratory burst frequency and dose-dependent increase in non-respiratory burst frequency. B) Top, continuous recording of CNX during perfusion of increasing doses of bicuculline in a preparation from a hibernated animal (blue). Bottom, zoomed in view of epochs (pink boxes) indicated in continuous trace above. Respiratory output from hibernated preparations was insensitive to system application of bicuculline, however non-respiratory motor bursting increased in a dose-dependent manner like controls. C) Summary of bicuculline-mediated changes in respiratory burst frequency. There was a significant interaction between drug and group by two-way ANOVA($F_{(4,32)}$=6.741; p=0.0005). Additionally, at 10 μM bicuculline, respiratory burst frequency from controls was significantly lower than hibernated preparations by Holm-Šidák's post-hoc test (p=0.0111; n=5/group). D) Summary of bicuculline-mediated changes in non-respiratory burst frequency. Bicuculline mediated similar increases in non-respiratory bursting in control and hibernated groups. There was no significant interaction between drug and group by two-way ANOVA ($F_{(4,32)}$=0.7948; p=0.5373; n=5/group). a.u., arbitrary units. In summary plots, thick lines represent the group average and thin lines are individual preparations.

Figure 2

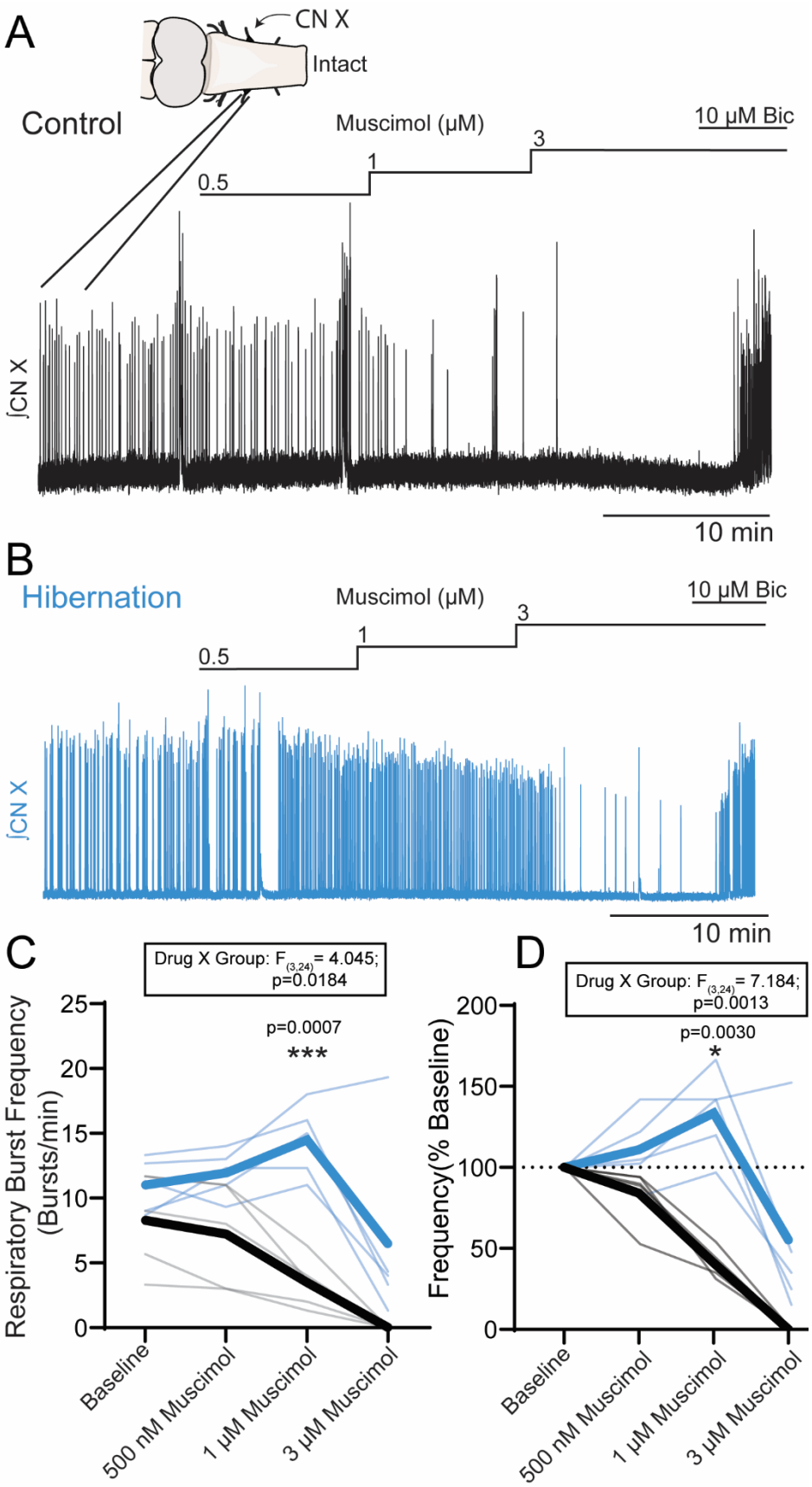
A
CN X
Intact
Control
Muscimol (μM)
10 μM Bic
0.5
1
3
∫CN X
10 min
B
Hibernation
Muscimol (μM)
10 μM Bic
0.5
1
3
∫CN X
10 min
C
Drug X Group: F(3,24) = 4.045; p=0.0184
p=0.0007
***
Respiratory Burst Frequency (Bursts/min)
25
20
15
10
5
0
Baseline
500 nM Muscimol
1 μM Muscimol
3 μM Muscimol
D
Drug X Group: F(3,24) = 7.184; p=0.0013
p=0.0030
*
Frequency(% Baseline)
200
150
100
50
0
Baseline
500 nM Muscimol
1 μM Muscimol
3 μM Muscimol

Figure 2

Hibernation decreases sensitivity to muscimol-mediated respiratory frequency decline. Integrated vagus nerve activity (CN X) was rhythmic in brainstem preparations from control and hibernated animals. A) Continuous recording of CNX during perfusion of increasing doses of muscimol in a control preparation (black). In control preparations, respiratory output was unchanged by bath application of 500nM muscimol but decreased following elevation to 1μM muscimol and ultimately stopped following further elevation to 3μM muscimol. B) Continuous recording of CNX during perfusion of increasing doses of muscimol in a preparation from a hibernated animal (blue). Preparations from hibernated animals were relatively insensitive to muscimol mediated changes in respiratory burst frequency compared to controls. C) Summary of muscimol-mediated changes in respiratory burst frequency. There was a significant interaction between drug and group by two-way ANOVA($F_{(3,24)}$=4.045; p=0.0184). Additionally, at 1 μM muscimol, respiratory burst frequency from controls was significantly lower than hibernated preparations by Holm-Šidák's post-hoc test (p=0.0007, n=5/group). D) Summary of muscimol-mediated changes in respiratory burst frequency relative to baseline. There was a significant interaction between drug and group by two-way ANOVA($F_{(3,24)}$=7.184; p=0.0013). Additionally, at 1 μM muscimol, respiratory burst frequency from controls was significantly lower than hibernated preparations relative to baseline by Šidák's post-hoc test (p=0.0030, n=5/group). In summary plots, thick lines represent the group average and thin lines are individual preparations.

Figure 3

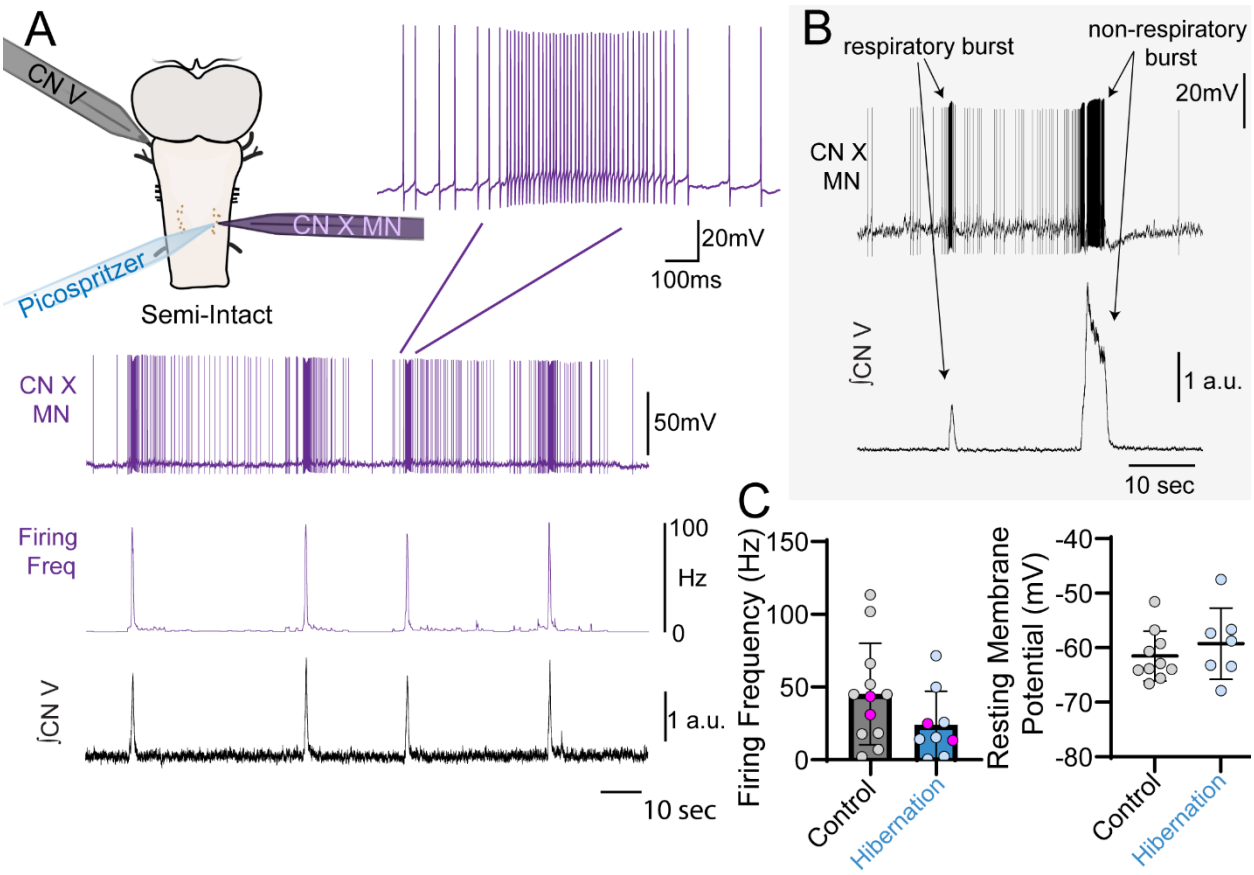
A
CN V
CN X MN
Picospritzer
Semi-Intact
20mV
100ms
CN X MN
50mV
Firing Freq
100
Hz
0
∫CN V
1 a.u.
10 sec
B
respiratory burst
non-respiratory burst
20mV
CN X MN
∫CN V
1 a.u.
10 sec
C
Firing Frequency (Hz)
150
100
50
0
Control
Hibernation
Resting Membrane Potential (mV)
-40
-50
-60
-70
-80
Control
Hibernation

Figure 3

Motoneuron firing in the semi-intact preparation is preserved following hibernation. Integrated trigeminal nerve activity (CN V) and whole-cell current clamp recordings of rhythmic vagal motor neurons (CN X MN) were recorded in the semi-intact brainstem preparation. A pipette driven by a Picospritzer was used to focally apply bicuculline onto the recorded vagal motor neuron in experiments. A) An example respiratory neuron (purple, top) fired rhythmic bursts, characterized by transient increases in firing frequency (purple, middle) during respiratory motor output (Black, bottom, CN V). B) An example vagal motor neuron fired in bursts during respiratory motor output as well as the occasional non-respiratory burst, suggesting these neurons participate in multiple behaviors. C) Baseline firing frequency of rhythmic respiratory neurons was not statistically different between control and hibernated groups by unpaired t-test ($p=0.1328$; $n= 12$ control cells; $n=9$ hibernated cells). Additionally, baseline resting membrane potential of rhythmic respiratory neurons was not statistically different between control and hibernated groups by unpaired t-test ($p=0.4094$; $n=10$ control cells; $n=7$ hibernated cells). Pink cells were recorded in loose-patch configuration. a.u., arbitrary units. Error bars are standard deviation (SD).

Figure 4

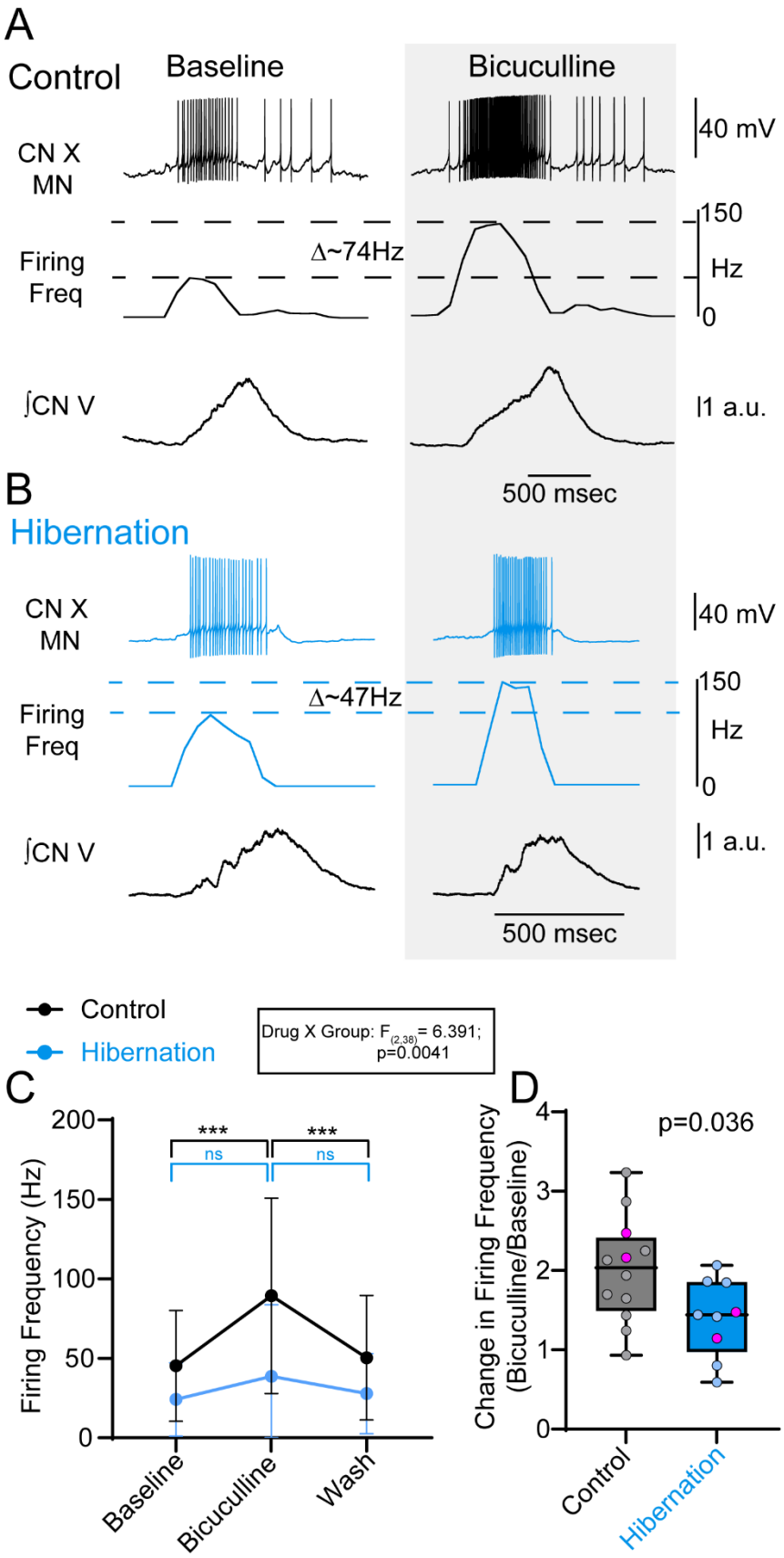
A
Control
Baseline
Bicuculline
CN X MN
40 mV
Firing Freq
Δ~74Hz
150
Hz
0
∫CN V
1 a.u.
500 msec
B
Hibernation
CN X MN
40 mV
Firing Freq
Δ~47Hz
150
Hz
0
∫CN V
1 a.u.
500 msec
Control
Hibernation
Drug X Group: F(2,38) = 6.391; p=0.0041
C
Firing Frequency (Hz)
200
150
100
50
0
***
ns
***
ns
Baseline
Bicuculline
Wash
D
Change in Firing Frequency (Bicuculline/Baseline)
p=0.036
4
3
2
1
0
Control
Hibernation

Figure 4

Hibernation decreases GABAergic inhibitory tone at the level of the respiratory motor neuron. A) Example respiratory motor activity in a control preparation (black). Example vagal motor neuron (CN X) fires bursts of action potentials during the respiratory burst (CN V). Focal application of bicuculline to the motor neuron increases burst firing frequency. B) Example respiratory motor activity in a preparation from a hibernated animal (blue). Example vagal motor neuron (CN X) also fired bursts of action potentials during the respiratory burst (CN V). Focal application of bicuculline to the motor neuron increased burst firing frequency, but not to the same extent as the control neuron. C) Summary of bicuculline-mediated increases in motor neuron firing frequency. There was a significant interaction between drug and group by two-way ANOVA ($F_{(2,38)}$=6.391; p=0.0041). Furthermore, there was a significant increase in burst firing frequency following focal application of bicuculline in control but not hibernated cells by Holm-Šidák's post-hoc test (***p<0.0001; n= 12 control cells; n=9 hibernated cells). D) Summary of bicuculline-mediated fold change in burst firing frequency from baseline. Control cells had a significantly larger bicuculline-mediated fold change in burst firing frequency than hibernated cells by unpaired t-test (p=0.036; ; n= 12 control cells; n=9 hibernated cells). Pink cells were recorded in loose-patch configuration. Box plots represent interquartile range and whiskers represent the minimum to maximum values. a.u., arbitrary units. Error bars are standard deviation (SD).

Figure 5

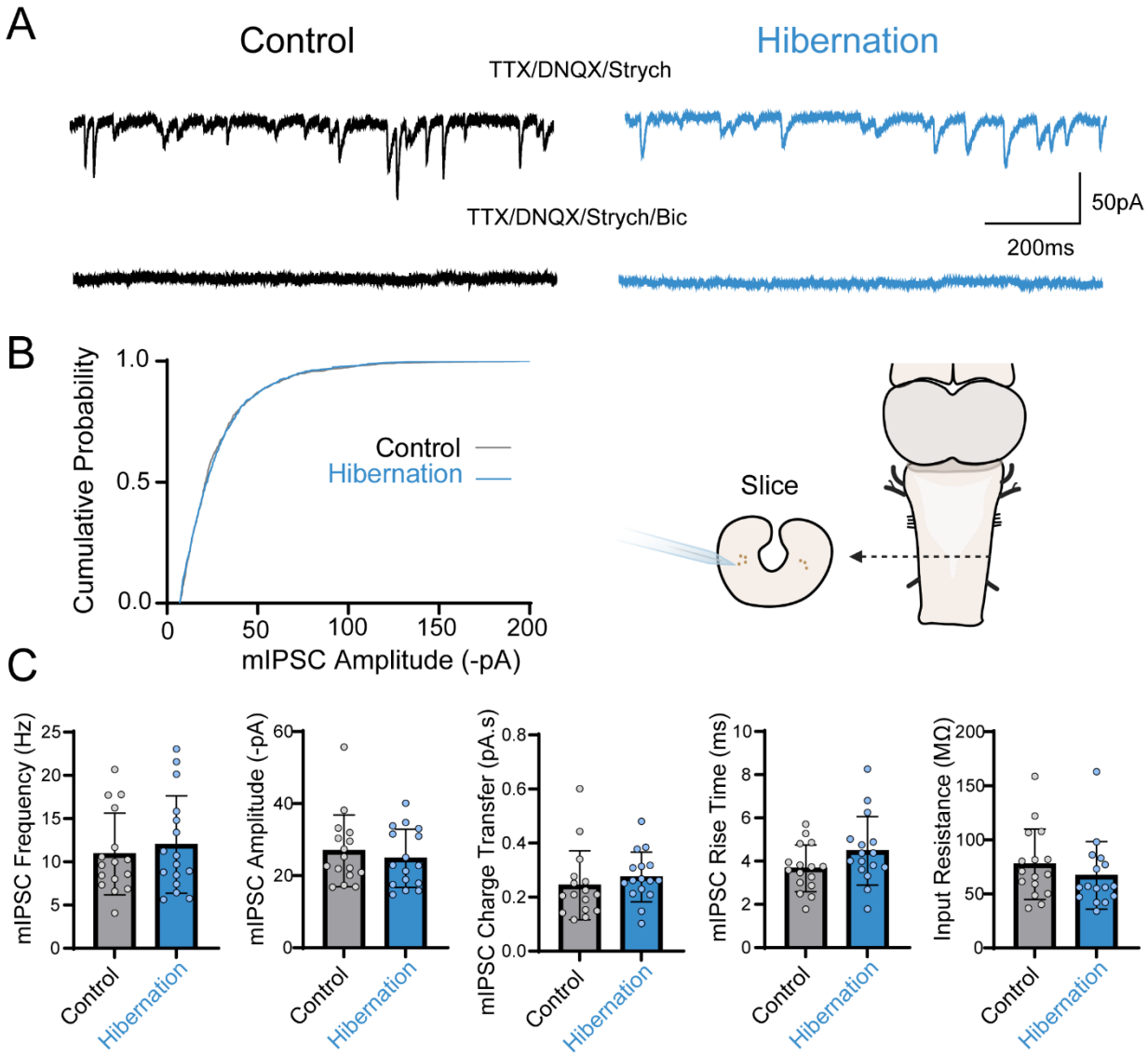
A
Control
Hibernation
TTX/DNQX/Strych
TTX/DNQX/Strych/Bic
50pA
200ms
B
Cumulative Probability
1.0
0.5
0.0
0
50
100
150
200
mIPSC Amplitude (-pA)
Control
Hibernation
Slice
C
mIPSC Frequency (Hz)
mIPSC Amplitude (-pA)
mIPSC Charge Transfer (pA.s)
mIPSC Rise Time (ms)
Input Resistance (MΩ)
Control
Hibernation

Figure 5

Motor neuron postsynaptic GABAergic inhibitory strength is unchanged following hibernation. A) Example voltage clamp traces of GABAergic miniature inhibitory postsynaptic currents (mIPSCs; holding potential = -60 mV; 250 nM TTX, 10 μM DNQX, 5 μM strychnine) from control (black) and hibernated (blue) identified vagal motor neurons in brain slice. Addition of 50 μM bicuculline to the bath eliminated mIPSCs in both groups, confirming GABAergic identity. B) Cumulative probability histograms of mIPSC amplitudes from control neurons (black line), hibernated neurons (blue line) appeared nearly identical. Accordingly, there was no statistical difference between distributions from control and hibernated cells by Kolomogorov-Smirnov test ($p = 0.5041$). C) Summary data. There was no statistical difference in mIPSC frequency, average amplitude, rise time, charge transfer and neuronal input resistance by unpaired t-test ($p > 0.05$; n= 16 control cells; n=16 hibernated cells). Error bars are standard deviation (SD).

References

Amaral-Silva, L. D., & Santin, J. M. (2022). A brainstem preparation allowing simultaneous access to respiratory motor output and cellular properties of motoneurons in American bullfrogs. *J. Exp. Biol.* 225(12), jeb244079. https://doi.org/10.1242/jeb.244079

Amaral-Silva, L., & Santin, J. M. (2023a). Synaptic modifications transform neural networks to function without oxygen. *BMC. Biol.* 21(1), 54. https://doi.org/10.1186/s12915-023-01518-0

Amaral-Silva, L., & Santin, J. M. (2023b). Molecular profiling of CO2/pH-sensitive neurons in the locus coeruleus of bullfrogs reveals overlapping noradrenergic and glutamatergic cell identity. *Comp. Biochem. Physiol. A. Mol. Integr. Physiol.* 283, 111453. https://doi.org/10.1016/j.cbpa.2023.111453

Anderson, T. M., Garcia, A. J., 3rd, Baertsch, N. A., Pollak, J., Bloom, J. C., Wei, A. D., Rai, K. G., & Ramirez, J. M. (2016). A novel excitatory network for the control of breathing. *Nature*. 536(7614), 76–80. https://doi.org/10.1038/nature18944

Baertsch, N. A., Baertsch, H. C., & Ramirez, J. M. (2018). The interdependence of excitation and inhibition for the control of dynamic breathing rhythms. *Nat. Commun.* 9(1), 843. https://doi.org/10.1038/s41467-018-03223-x

Baertsch, N. A., & Baker-Herman, T. L. (2013). Inactivity-induced phrenic and hypoglossal motor facilitation are differentially expressed following intermittent vs. sustained neural apnea. *J. Appl. Physiol.* (Bethesda, Md. : 1985), 114(10), 1388–1395. https://doi.org/10.1152/japplphysiol.00018.2013

Baghdadwala, M. I., Duchcherer, M., Paramonov, J., & Wilson, R. J. (2015). Three brainstem areas involved in respiratory rhythm generation in bullfrogs. *J. Physiol.* 593(13), 2941–2954. https://doi.org/10.1113/JP270380

Baghdadwala, M. I., Duchcherer, M., Trask, W. M., Gray, P. A., & Wilson, R. J. (2016). Diving into the mammalian swamp of respiratory rhythm generation with the bullfrog. *Respir. Physiol. Neurobiol.* 224, 37–51. https://doi.org/10.1016/j.resp.2015.09.005

Baker-Herman, T. L., Fuller, D. D., Bavis, R. W., Zabka, A. G., Golder, F. J., Doperalski, N. J., Johnson, R. A., Watters, J. J., & Mitchell, G. S. (2004). BDNF is necessary and sufficient for spinal respiratory plasticity following intermittent hypoxia. *Nat. Neurosci.* 7(1), 48–55. https://doi.org/10.1038/nn1166

Baker-Herman, T. L., & Mitchell, G. S. (2008). Determinants of frequency long-term facilitation following acute intermittent hypoxia in vagotomized rats. *Respir. Physiol. Neurobiol.* 162(1), 8–17. https://doi.org/10.1016/j.resp.2008.03.005

Banzrai, C., Nodera, H., Kawarai, T., Higashi, S., Okada, R., Mori, A., Shimatani, Y., Osaki, Y., & Kaji, R. (2016). Impaired Axonal Na(+) Current by Hindlimb Unloading:

Implication for Disuse Neuromuscular Atrophy. *Front. Physiol.* 7, 36. https://doi.org/10.3389/fphys.2016.00036

Barberis, A., Petrini, E. M., & Cherubini, E. (2004). Presynaptic source of quantal size variability at GABAergic synapses in rat hippocampal neurons in culture. *Eur. J. Neurosci.* 20(7), 1803–1810. https://doi.org/10.1111/j.1460-9568.2004.03624.x

Barnett, W. H., Jenkin, S. E. M., Milsom, W. K., Paton, J. F. R., Abdala, A. P., Molkov, Y. I., & Zoccal, D. B. (2018). The Kölliker-Fuse nucleus orchestrates the timing of expiratory abdominal nerve bursting. *J. Neurophysiol.* 119(2), 401–412. https://doi.org/10.1152/jn.00499.2017

Benevento, L. A., Bakkum, B. W., & Cohen, R. S. (1995). gamma-Aminobutyric acid and somatostatin immunoreactivity in the visual cortex of normal and dark-reared rats. *Brain. Res*. 689(2), 172–182. https://doi.org/10.1016/0006-8993(95)00553-3

Blitz, D. M., & Ramirez, J. M. (2002). Long-term modulation of respiratory network activity following anoxia in vitro. *J. Neurophysiol.* 87(6), 2964–2971. https://doi.org/10.1152/jn.2002.87.6.2964

Bongianni, F., Mutolo, D., Nardone, F., & Pantaleo, T. (2006). GABAergic and glycinergic inhibitory mechanisms in the lamprey respiratory control. *Brain. Res.* 1090(1), 134–145. https://doi.org/10.1016/j.brainres.2006.03.056

Bongianni, F., Mutolo, D., Cinelli, E., & Pantaleo, T. (2016). Neural mechanisms underlying respiratory rhythm generation in the lamprey. *Respir. Physiol. Neurobiol.* 224, 17–26. https://doi.org/10.1016/j.resp.2014.09.003

Braegelmann, K. M., Streeter, K. A., Fields, D. P., & Baker, T. L. (2017). Plasticity in respiratory motor neurons in response to reduced synaptic inputs: A form of homeostatic plasticity in respiratory control?. *Exp. Neurol*. 287(Pt 2), 225–234. https://doi.org/10.1016/j.expneurol.2016.07.012

Briggman, K. L., & Kristan, W. B. (2008). Multifunctional pattern-generating circuits. *Annu. Rev. Neurosci.* 31, 271–294. https://doi.org/10.1146/annurev.neuro.31.060407.125552

Broch, L., Morales, R. D., Sandoval, A. V., & Hedrick, M. S. (2002). Regulation of the respiratory central pattern generator by chloride-dependent inhibition during development in the bullfrog (Rana catesbeiana). *J. Exp. Biol.* 205 (8): 1161–1169. https://doi.org/10.1242/jeb.205.8.1161

Brockhaus, J., & Ballanyi, K. (2000). Anticonvulsant A(1) receptor-mediated adenosine action on neuronal networks in the brainstem-spinal cord of newborn rats. *Neuroscience.* 96(2), 359–371. https://doi.org/10.1016/s0306-4522(99)00544-8

Burggren W. W. (2020). Phenotypic Switching Resulting From Developmental Plasticity: Fixed or Reversible?. *Front. Physiol.* 10, 1634. https://doi.org/10.3389/fphys.2019.01634

Burton, M. T., & Santin, J. M. (2020). A direct excitatory action of lactate ions in the central respiratory network of bullfrogs, Lithobates catesbeianus. *J. Exp. Biol*. 223(Pt 24), jeb235705. https://doi.org/10.1242/jeb.235705

Büsselberg, D., Bischoff, A. M., Paton, J. F., & Richter, D. W. (2001). Reorganisation of respiratory network activity after loss of glycinergic inhibition. *Pflugers. Arch.* 441(4), 444–449. https://doi.org/10.1007/s004240000453

Cormery, B., Beaumont, E., Csukly, K., & Gardiner, P. (2005). Hindlimb unweighting for 2 weeks alters physiological properties of rat hindlimb motoneurones. *J. Physiol*. 568(Pt 3), 841–850. https://doi.org/10.1113/jphysiol.2005.091835

Cregg, J. M., Chu, K. A., Dick, T. E., Landmesser, L. T., & Silver, J. (2017). Phasic inhibition as a mechanism for generation of rapid respiratory rhythms. *Proc. Natl. Acad. Sci. U. S. A.* 114(48), 12815–12820. https://doi.org/10.1073/pnas.1711536114

Cui, Y., Kam, K., Sherman, D., Janczewski, W. A., Zheng, Y., & Feldman, J. L. (2016). Defining preBötzinger Complex Rhythm- and Pattern-Generating Neural Microcircuits In Vivo. *Neuron*. 91(3), 602–614. https://doi.org/10.1016/j.neuron.2016.07.003

Delhaes, F., Fournier, S., Tolsa, J. F., Peyter, A. C., Bairam, A., & Kinkead, R. (2014). Consequences of gestational stress on GABAergic modulation of respiratory activity in developing newborn pups. *Respir. Physiol. Neurobiol.* 200, 72–79. https://doi.org/10.1016/j.resp.2014.05.015

Dempsey, J. A., & Morgan, B. J. (2015). Humans In Hypoxia: A Conspiracy Of Maladaptation?!. *Physiology (Bethesda, Md.),* 30(4), 304–316. https://doi.org/10.1152/physiol.00007.2015

Fahim M. A. (1989). Rapid neuromuscular remodeling following limb immobilization. *Anat. Rec*. 224(1), 102–109. https://doi.org/10.1002/ar.1092240113

Fong, M. F., Newman, J. P., Potter, S. M., & Wenner, P. (2015). Upward synaptic scaling is dependent on neurotransmission rather than spiking. *Nat. Commun*. 6, 6339. https://doi.org/10.1038/ncomms7339

Hanamori, T., Ishiko, N., & Smith, D. V. (1987). Multimodal responses of taste neurons in the frog nucleus tractus solitarius. *Brain. Res. Bull.* 18(1), 87–97. https://doi.org/10.1016/0361-9230(87)90036-0

Hartman, K. N., Pal, S. K., Burrone, J., & Murthy, V. N. (2006). Activity-dependent regulation of inhibitory synaptic transmission in hippocampal neurons. *Nat. Neurosci.* 9(5), 642–649. https://doi.org/10.1038/nn1677

Hendry, S. H., & Jones, E. G. (1986). Reduction in number of immunostained GABAergic neurones in deprived-eye dominance columns of monkey area 17. *Nature*. 320(6064), 750–753. https://doi.org/10.1038/320750a0

Hendry, S. H., & Jones, E. G. (1988). Activity-dependent regulation of GABA expression in the visual cortex of adult monkeys. *Neuron*. 1(8), 701–712. https://doi.org/10.1016/0896-6273(88)90169-9

Hendry, S. H., Huntsman, M. M., Viñuela, A., Möhler, H., de Blas, A. L., & Jones, E. G. (1994). GABAA receptor subunit immunoreactivity in primate visual cortex: distribution in macaques and humans and regulation by visual input in adulthood. *J. Neurosci.* 14(4), 2383–2401. https://doi.org/10.1523/JNEUROSCI.14-04-02383.1994

Jaiswal, S. J., Wollman, L. B., Harrison, C. M., Pilarski, J. Q., & Fregosi, R. F. (2016). Developmental nicotine exposure enhances inhibitory synaptic transmission in motor neurons and interneurons critical for normal breathing. *Dev. Neurobiol.* 76(3), 337–354. https://doi.org/10.1002/dneu.22318

Janczewski, W. A., Tashima, A., Hsu, P., Cui, Y., & Feldman, J. L. (2013). Role of inhibition in respiratory pattern generation. J. Neurosci. 33(13), 5454–5465. https://doi.org/10.1523/JNEUROSCI.1595-12.2013

Johnson, S. M., Wilkerson, J. E., Wenninger, M. R., Henderson, D. R., & Mitchell, G. S. (2002). Role of synaptic inhibition in turtle respiratory rhythm generation. *J. Physiol.* 544(Pt 1), 253–265. https://doi.org/10.1113/jphysiol.2002.019687

Kahn, A., Groswasser, J., Sottiaux, M., Kelmanson, I., Rebuffat, E., Franco, P., Dramaix, M., & Wayenberg, J. L. (1994). Prenatal exposure to cigarettes in infants with obstructive sleep apneas. Pediatrics, 93(5), 778–783.

Khristy, W., Ali, N. J., Bravo, A. B., de Leon, R., Roy, R. R., Zhong, H., London, N. J., Edgerton, V. R., & Tillakaratne, N. J. (2009). Changes in GABA(A) receptor subunit gamma 2 in extensor and flexor motoneurons and astrocytes after spinal cord transection and motor training. *Brain. Res.* 1273, 9–17. https://doi.org/10.1016/j.brainres.2009.03.060

Kilman, V., van Rossum, M. C., & Turrigiano, G. G. (2002). Activity deprivation reduces miniature IPSC amplitude by decreasing the number of postsynaptic GABA(A) receptors clustered at neocortical synapses. *J. Neurosci.* 22(4), 1328–1337. https://doi.org/10.1523/JNEUROSCI.22-04-01328.2002

Kim, J., & Tsien, R. W. (2008). Synapse-specific adaptations to inactivity in hippocampal circuits achieve homeostatic gain control while dampening network reverberation. *Neuron*. 58(6), 925–937. https://doi.org/10.1016/j.neuron.2008.05.009

Kimura, N., Perry, S. F., & Remmers, J. E. (1997). Strychnine eliminates reciprocation and augmentation of respiratory bursts of the in vitro frog brainstem. *Neurosci. Lett*. 225(1), 9–12. https://doi.org/10.1016/s0304-3940(97)00171-7

Kogo, N., Perry, S. F., & Remmers, J. E. (1994). Neural organization of the ventilatory activity in the frog, Rana catesbeiana. I. *J. Neurobiol.* 25(9), 1067–1079. https://doi.org/10.1002/neu.480250904

Kogo, N., & Remmers, J. E. (1994). Neural organization of the ventilatory activity in the frog, Rana catesbeiana. II. *J. Neurobiol.* 25(9), 1080–1094. https://doi.org/10.1002/neu.480250905

Langlet, C., Bastide, B., & Canu, M. H. (2012). Hindlimb unloading affects cortical motor maps and decreases corticospinal excitability. *Exp. Neurol*. 237(1), 211–217. https://doi.org/10.1016/j.expneurol.2012.06.018

Lambo, M. E., & Turrigiano, G. G. (2013). Synaptic and intrinsic homeostatic mechanisms cooperate to increase L2/3 pyramidal neuron excitability during a late phase of critical period plasticity. *J. Neurosci.* 33(20), 8810–8819. https://doi.org/10.1523/JNEUROSCI.4502-12.2013

Mahamed, S., Strey, K. A., Mitchell, G. S., & Baker-Herman, T. L. (2011). Reduced respiratory neural activity elicits phrenic motor facilitation. *Respir. Physiol. Neurobiol.* 175(3), 303–309. https://doi.org/10.1016/j.resp.2010.12.005

Mitchell, G. S., Baker, T. L., Nanda, S. A., Fuller, D. D., Zabka, A. G., Hodgeman, B. A., Bavis, R. W., Mack, K. J., & Olson, E. B., Jr (2001). Invited review: Intermittent hypoxia and respiratory plasticity. *J. Appl. Physiol.* (Bethesda, Md. : 1985), 90(6), 2466–2475. https://doi.org/10.1152/jappl.2001.90.6.2466

Pace, R. W., & Del Negro, C. A. (2008). AMPA and metabotropic glutamate receptors cooperatively generate inspiratory-like depolarization in mouse respiratory neurons in vitro. *Eur. J. Neurosci.* 28(12), 2434–2442. https://doi.org/10.1111/j.1460-9568.2008.06540.x

Panaitescu, B., Kuribayashi, J., Ruangkittisakul, A., Leung, V., Iizuka, M., & Ballanyi, K. (2013). Methylxanthines do not affect rhythmogenic preBötC inspiratory network activity but impair bursting of preBötC-driven motoneurons. *Neuroscience.* 255, 158–176. https://doi.org/10.1016/j.neuroscience.2013.09.058

Paulose, C. S., John, P. S., Sreekanth, R., Philip, M., Mohan, C. P., Mathew, J., Kumar, T. P., Paul, J., Abraham, P. M., Antony, S., Joseph, B., Joseph, A., Krishnakumar, A., Anju, T. R., Khan, S. R., Thomas, K. S., & Nandhu, M. S. (2009). Spinal cord regeneration and functional recovery: neurotransmitter's combination and bone marrow cells supplementation. *Curr. Sci.* 97(4), 546–549. http://www.jstor.org/stable/24111883

Peng, Y. R., Zeng, S. Y., Song, H. L., Li, M. Y., Yamada, M. K., & Yu, X. (2010). Postsynaptic spiking homeostatically induces cell-autonomous regulation of inhibitory inputs via retrograde signaling. *J. Neurosci.* 30(48), 16220–16231. https://doi.org/10.1523/JNEUROSCI.3085-10.2010

Pilarski, J. Q., & Fregosi, R. F. (2009). Prenatal nicotine exposure alters medullary nicotinic and AMPA-mediated control of respiratory frequency in vitro. *Respir. Physiol. Neurobiol.* 169(1), 1–10. https://doi.org/10.1016/j.resp.2009.07.022

Rutherford, L. C., DeWan, A., Lauer, H. M., & Turrigiano, G. G. (1997). Brain-derived neurotrophic factor mediates the activity-dependent regulation of inhibition in neocortical cultures. *J. Neurosci*. 17(12), 4527–4535. https://doi.org/10.1523/JNEUROSCI.17-12-04527.1997

Sakakibara Y. (1984). The pattern of respiratory nerve activity in the bullfrog. *Jpn. J. Physiol.* 34(2), 269–282. https://doi.org/10.2170/jjphysiol.34.269

Santin, J. M., & Hartzler, L. K. (2013). Respiratory signaling of locus coeruleus neurons during hypercapnic acidosis in the bullfrog, Lithobates catesbeianus. *Respir. Physiol. Neurobiol*. 185(3), 553–561. https://doi.org/10.1016/j.resp.2012.11.002

Santin, J. M., & Hartzler, L. K. (2016). Environmentally induced return to juvenile-like chemosensitivity in the respiratory control system of adult bullfrog, Lithobates catesbeianus. *J. Physiol.* 594(21), 6349–6367. https://doi.org/10.1113/JP272777

Santin, J. M., & Hartzler, L. K. (2017). Activation of respiratory muscles does not occur during cold-submergence in bullfrogs, Lithobates catesbeianus. *J. Exp. Biol.* 220(Pt 7), 1181–1186. https://doi.org/10.1242/jeb.153544

Santin, J. M., Vallejo, M., & Hartzler, L. K. (2017). Synaptic up-scaling preserves motor circuit output after chronic, natural inactivity. *eLife*. 6, e30005. https://doi.org/10.7554/eLife.30005

Santin J. M. (2019). Motor inactivity in hibernating frogs: Linking plasticity that stabilizes neuronal function to behavior in the natural environment. *Dev. Neurobiol*. 79(9-10), 880–891. https://doi.org/10.1002/dneu.22721

Smuder, A. J., Levine, S., & Powers, S. K. (2023). Critical Illness Myopathy Alters Diaphragm Neuromuscular Junction Protein and Gene Expression. *Am. J. Respir. Crit. Care. Med.* 207(3), 358–361. https://doi.org/10.1164/rccm.202204-0683LE

Streeter, K. A., & Baker-Herman, T. L. (2014). Decreased spinal synaptic inputs to phrenic motor neurons elicit localized inactivity-induced phrenic motor facilitation. *Exp. Neuro.* 256, 46–56. https://doi.org/10.1016/j.expneurol.2014.03.007

Sun, Q. J., Berkowitz, R. G., & Pilowsky, P. M. (2008). GABA A mediated inhibition and post-inspiratory pattern of laryngeal constrictor motoneurons in rat. *Respir. Physiol. Neurobiol.* 162(1), 41–47. https://doi.org/10.1016/j.resp.2008.03.013

Swanwick, C. C., Murthy, N. R., & Kapur, J. (2006). Activity-dependent scaling of GABAergic synapse strength is regulated by brain-derived neurotrophic factor. *Mol. Cell. Neurosci.* 31(3), 481–492. https://doi.org/10.1016/j.mcn.2005.11.002

Turrigiano, G. G., Leslie, K. R., Desai, N. S., Rutherford, L. C., & Nelson, S. B. (1998). Activity-dependent scaling of quantal amplitude in neocortical neurons. *Nature*. 391(6670), 892–896. https://doi.org/10.1038/36103

Vincen-Brown, M. A., Revill, A. L., & Pilarski, J. Q. (2016). Activity-dependent plasticity in the isolated embryonic avian brainstem following manipulations of rhythmic spontaneous neural activity. *Respir. Physiol. Neurobiol.* 229, 24–33. https://doi.org/10.1016/j.resp.2016.03.013

Wang, T., Hedrick, M. S., Ihmied, Y. M., & Taylor, E. W. (1999). Control and interaction of the cardiovascular and respiratory systems in anuran amphibians. *Comp. Biochem. Physiol. A. Mol. Integr. Physiol*. 124(4), 393–406. https://doi.org/10.1016/s1095-6433(99)00131-2

Wilson, R. J., Vasilakos, K., Harris, M. B., Straus, C., & Remmers, J. E. (2002). Evidence that ventilatory rhythmogenesis in the frog involves two distinct neuronal oscillators. *J Physiol.* 540(Pt 2), 557–570. https://doi.org/10.1113/jphysiol.2001.013512

Wollman, L. B., Flanigan, E. G., & Fregosi, R. F. (2022). Chronic, episodic nicotine exposure alters GABAergic synaptic transmission to hypoglossal motor neurons and genioglossus muscle function at a critical developmental age. *J. Neurophysiol.* 128(6), 1483–1500. https://doi.org/10.1152/jn.00397.2022

Wollman, L. B., Levine, R. B., & Fregosi, R. F. (2018). Developmental plasticity of GABAergic neurotransmission to brainstem motoneurons. *J. Physiol.* 596(23), 5993–6008. https://doi.org/10.1113/JP274923

Zubov, T., do Amaral-Silva, L., & Santin, J. M. (2022). Inactivity and Ca2+ signaling regulate synaptic compensation in motoneurons following hibernation in American bullfrogs. *Sci. Rep*. 12(1), 11610. https://doi.org/10.1038/s41598-022-15525-8

Zuperku, E. J., & McCrimmon, D. R. (2002). Gain modulation of respiratory neurons. *Respir. Physiol. Neurobiol. 131*(1-2), 121–133. https://doi.org/10.1016/s1569-9048(02)00042-3